Solitary Waves and Fluctuations in Fragile Matter

Upadhyaya, N.

4

FLUCTUATIONS AND EMERGENT PROPERTIES

The simple model that we have used to understand the regime of exponential decay of the solitary wave amplitude (for weak disorder) suggests that at each subsequent collision with an inhomogeneity, the solitary wave splits approximately into two solitary waves- a leading pulse (the main degree of freedom that is damped exponentially as a result) and a smaller solitary wave, that is either reflected or transmitted depending upon the mass ratio *. Therefore, once we allow sufficient time for the leading solitary wave to disintegrate completely such that a leading pulse is no longer distinguishable from the background, we expect to reach a state comprised of several smaller solitary waves with different energies, see Fig. (4.1)(bottom). The solitary waves in turn interact with each other in-elastically, (as a consequence of the Nesterenko equation of motion being non-integrable [6]) and thus their interaction may be thought of as inherently dissipative. However, in addition to these processes that seek to distribute the energy initially concentrated in a single solitary wave excitation into multiple smaller solitary waves, the structural disorder in two dimensional amorphous packings also spills a part of the energy into transverse degrees of motion. Through a series of such intrinsic dissipative mechanisms, we eventually reach a fluctuating equilibrium-like state that spans the entire finite-sized packings under-investigation.

4.1 VIRIAL RELATION

As a check to demonstrate the emergence of an equilibirum like state, we compute the distribution of energies between the kinetic and potential degrees of freedom - the Virial relation. We first recall the Virial relation for a general (non) linear oscillator.

Consider a one dimensional oscillator whose Hamiltonian is

$$H = \frac{p^2}{(2m)} + q^{\alpha}, \tag{4.1}$$

* Here, we are sidestepping the question pertaining to the identity of the transmitted solitary wave, i.e., whether it is a new solitary wave with a smaller amplitude or the old one that has been attenuated

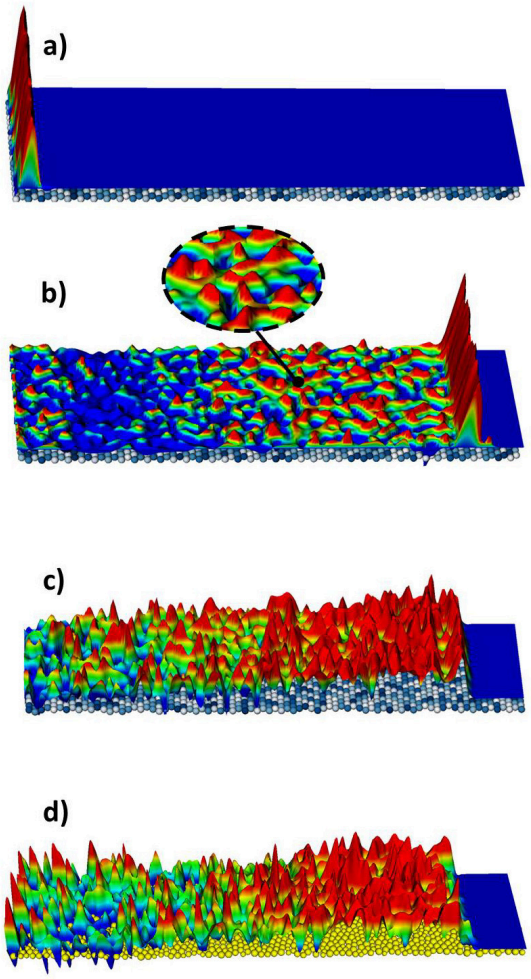

Figure 4.1: (a) A schematic illustration of how a hexagonal packing at zero pressure (with vanishing longitudinal and transverse sound speeds) and weak mass disorder, responds to an impact at one of its ends, by generating a solitary wave excitation. (b) As the solitary wave propagates and interacts with the weak mass inhomogeneity, its amplitude decays. The decay at early times is nearly exponential and the process of energy loss is such, that it excites several smaller solitary waves. Over the long run, a noisy state (velocity fluctuations) spanning the size of the packing emerges (zoomed region). (c) The initial solitary wave is now no longer identifiable in a hexagonal packing with strong mass disorder. Instead we observe a triangular shock like profile that is defined as an envelope over the smaller excitations. In this regime, the decay of the leading edge follows a power law. Eventually, no leading propagating edge is visible. (d) Similar to the strongly disordered hexagonal packing, no initial solitary wave is seen in a jammed amorphous packing. Instead, an impulse excitation soon evolves into the universal triangular shock-like profile. These plots, show the particle velocity field where the front amplitudes and positions have been rescaled for better illustration.

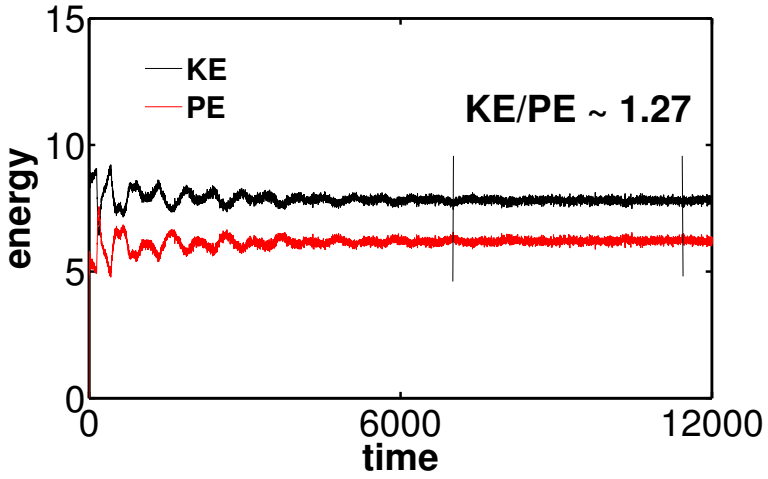

Figure 4.2: The virial relation in the quasi-equilibirum state showing the ratio between kinetic energy (KE) and potential energy (PE) to be approximately KE/PE≈1.27.

where, p, q are the generalized momentum and position coordinates. The equipartition theorem states that under suitable assumptions of thermal equilibrium, the following is satisfied:

$$\left\langle x_n \frac{\partial H}{\partial x_n} \right\rangle = k_B T \tag{4.2}$$

where $x_n = p, q$ is a generalized coordinate. Thus, $\frac{p^2}{m} = k_B T$ and $\alpha q^\alpha = k_B T$. Therefore, the kinetic energy is KE=$\frac{p^2}{(2m)} = \frac{k_B T}{2}$ and the potential energy is PE=$q^\alpha = \frac{k_B T}{\alpha}$ with their ratio being KE/PE=$\frac{\alpha}{2}$.

For the harmonic oscillator, $\alpha = 2$ and thus, we recover the usual equipartition of energy between quadratic degrees of freedom. However, for a non-linear oscillator, say of the Hertz form considered previously, the corresponding ratio is $\frac{5}{4}$. In other words, on an average the kinetic energy is greater than the potential energy for $\alpha > 2$. Intuitively, for $\alpha > 2$ and small displacements from equilibrium, the non-linear return force is weaker (or the potential is said to be softer) than for the corresponding harmonic oscillator. Thus, such a particle is “free" more of the time, and consequently, has a higher kinetic energy.

In Fig. (4.2), we verify this relation in the asymptotic state that an amorphous packing reaches, once we allow sufficient time for the initial impulse excitation to no longer be identifiable. We find that in this state, the ratio of kinetic and potential energies, does indeed approach the Virial limit. Recall, all model

systems we have considered so far, represent macroscopic objects in contact and a-priori, temperature is not a relevant variable. However, the agitations induced by the decaying solitary wave cause the packing of frictionless disks to acquire a state, that mimics an equilibrium like state, where the initial solitary wave energy plays the role of temperature (although not truly in thermal equilibrium).

4.2 HYDRODYNAMICAL MODES

In order to rationalize the physics behind this fluctuating state that at first appears to be just noise (see Fig. (4.1), bottom panels), we assume the existence of small wave-number k and small frequency ω, longitudinal (l) and transverse (t) hydrodynamical modes and obtain their power spectral densities, as follows.

In order to obtain hydrodynamical modes from the velocity field of fluctuating particles, we use the statistical mechanical definition of particle current density, defined as

$$\mathbf{j}(\mathbf{r}, t) = \frac{1}{\sqrt{N}} \sum_{i=1}^{N} \mathbf{v}_i(t)\delta(\mathbf{r} - \mathbf{r}_i(t)), \tag{4.3}$$

where, N is the number of particles and bold-face variables correspond to two dimensional Cartesian coordinates. The Fourier transform of the Cartesian component α, is given by

$$j_\alpha(\mathbf{k}, t) = \frac{1}{\sqrt{N}} \sum_{i=1}^{N} v_{i\alpha}(t) e^{i\mathbf{k}\cdot\mathbf{r}_i(t)}. \tag{4.4}$$

Assuming now, that the hydrodynamical collective modes propagate along the x-direction (assumed isotropy of the amorphous packing) , i.e., $\mathbf{k} = (k, 0)$, we let $\alpha = x$ or y, which allows us to define the corresponding longitudinal or transverse current density auto-correlation functions as

$$C_{l,t}(k, t) = \langle j^*_{l,t}(\mathbf{k}, 0) j_{l,t}(\mathbf{k}, t)\rangle, \tag{4.5}$$

where the angular brackets denote ensemble averaging over the initial time. The longitudinal/transverse spectral densities are then obtained as the Fourier transform of the respective current density auto-correlation functions as,

$$P_{l,t}(k, \omega) = \int_{-\infty}^{\infty} dt\ e^{i\omega t} C_{l,t}(k, t). \tag{4.6}$$

The Fourier transforms defined in Eq. (4.6) are evaluated using Fast Fourier transform from simulation data.

Within the linearized hydrodynamical description, the longitudinal power spectral density is of the form (see Supplementary Information C for a detailed derivation)

$$P_l \propto \frac{\omega^2 \eta k^2}{\left[\omega^2 - \omega_0^2\right]^2 + (\omega \eta k^2)^2}, \tag{4.7}$$

while the transverse power spectral density is of the form

$$P_t \propto \frac{\eta k^2}{\omega^2 + (\eta k^2)^2}. \tag{4.8}$$

Here, η is the coefficient of viscosity in the Navier-Stokes equation and $\omega_0 = ck$ is the linear longitudinal dispersion curve, where c is the speed of sound. Thus, the longitudinal modes (or current fluctuations) propagate at the speed of sound (obtained from the linear dispersion relation) and are damped by viscous effects, manifest in the half-width at half-maximum of the power spectral density that scales as h.w.$\sim \eta k^2$. On the other hand, the transverse modes are non-propagating, but instead, are damped exponentially in time, at a rate equal to ηk^2, which is also its half-width at half-maximum. This coincides with our intuitive understanding, that fluids have a finite bulk modulus (longitudinal sound speed), but no shear modulus.

Shown in Fig. (4.3), right panel (b), are the longitudinal (red squares) and transverse (red circles) dispersion curves that are obtained numerically by projecting the respective power spectral densities (Fig. (4.3) right panel (a)) into the $k-\omega$ plane. For comparison are shown, the corresponding longitudinal (black squares) and transverse (black circles) dispersion curves for a highly compressed jammed packing far from the critical density, prepared at a pressure of $P\sim 10^{-1}$. Since the total potential energy of a jammed packing is related to its pressure via $E\sim P^{\frac{5}{3}}$, the numerical data shown for the emergent state, corresponds to an impact speed $U_p \approx 2.0$ in order to generate a solitary wave in the weakly compressed packings ($P\sim 10^{-6}$) with an energy E_{SW} that is comparable to the energy of the highly compressed packing E_{PC} to facilitate a more meaningful comparison between the two states.

As seen in Fig. (4.3) right panel (b), highly compressed jammed packings behave as ordinary solids with a finite bulk and shear modulus and this translates into a finite sound speed manifest in the linear regime of the longitudinal (black squares)

and shear (black circles) dispersion curves. In contrast, exciting a jammed packing prepared at a vanishingly small pressures (that a-priori has nearly zero longitudinal and shear sound speeds), leads to a linear dispersion regime for the longitudinal modes, but no such regime is obtained for the transverse modes. The slope of the linear regime in the longitudinal dispersion curves, corresponds to the speed of long wavelength hydrodynamical sound modes. Defining the sound speed c as the second derivative of the induced potential energy; E_{SW}; leads to the relation, $c \sim E_{SW}^{\frac{1}{10}}$ [38], closely matching the numerical data in Inset to Fig. (4.3) right panel (b), red squares. Thus, the speed of the long wavelength hydrodynamical sound modes scales with the energy of the initial solitary wave E_{SW} injected into the system [45].

This is analogous to the scaling relation for pre-compressed jammed packings at a finite packing fraction δ_0, where the sound speed is found to scale as $c \sim E_{PC}^{\frac{1}{10}}$, with E_{PC} being the potential energy due to the finite pre-compression δ_0. Thus, in so far as longitudinal sound modes are concerned, a rigidity induced by statically compressing a marginally compressed packing is analogous to the rigidity induced by exciting a marginally compressed packing with a finite energy wave. Note therefore, one can easily replace the source of energy by a heat bath and thereby obtain a thermally induced rigidity upon making the substitution $E \rightarrow k_B T$. However, unlike a state that is truly in thermal equilibrium, an external perturbation over the fluctuating state created by the disintegration of a solitary wave, will further raise its energy due to the absence of a fluctuation-dissipation mechanism. The emergent state is thus at best described as a quasi-equilibrium state.

Fluidization of the jammed packing endows it with a finite bulk modulus.

In contrast to the longitudinal modes, the transverse modes obtained by energizing a marginally compressed packing do not show a well defined linear regime, see Fig. (4.3) right panel (b), red circles. This is in stark contrast from a statically compressed jammed packing where a linear transverse dispersion regime (owing to the finite shear modulous) with a slope that scales with the amount of pre-compression (and does not depend upon the solitary wave energy injected) as $c \sim E_{PC}^{\frac{1}{5}}$ is expected (Fig. (4.3) right panel (b), black circles). Thus, the shear modes excited by injecting energy into a packing near its critical point are purely diffusive and the medium does not develop a finite shear modulus. There is therefore a profound dif-

ference between the resultant states obtained by (a) statically compressing a granular packing near its critical point versus (b) injecting energy either in the form of an excitation or thermally. In the former case, one obtains a solid-like medium with finite bulk and shear moduli, while in the latter, we fluidize the medium. This means that, even after the non-linear wave excitations (characteristic of the jamming point) are strongly attenuated, one cannot describe the system purely in terms of the normal modes of a (linear elastic) solid because the system has *de facto* become a fluid. This is one of the key conclusions of this work and it heralds the signature property of packings at the jamming threshold: they are fragile. See also Chapter 6, where we find that the initial response (below a length scale) of a fragile network of harmonic springs is independent of the details of the network connectivity and does not contain any propagating modes.

In Fig. (4.3) right panel (c), we show how the half width (inverse lifetime τ) of the longitudinal hydrodynamical modes depends anomalously upon the wavenumber as $\tau^{-1} \sim k^{1.6}$. For purely hydrodynamical modes obeying the Navier-Stokes equation, the half width scales with the wave number as $hw \sim \eta k^2$, where η is the shear viscosity, see Eq. (4.7). However, extensive numerical and analytical studies have shown that in one dimension the time correlation functions (whose long time integrals by definition correspond to macroscopic transport properties such as diffusivity and shear viscosity) do not decay exponentially but display long time tails, decaying as power laws instead [40, 41, 42].

This phenomenon indicates the breakdown in low dimensions of the standard mean field approximation embedded in the Navier-Stokes equation – the strength of fluctuations is too strong for simple coarse-grained theories to hold. Note, the Navier-Stokes equation is conventionally expressed without any fluctuating noise term. For three and two dimensional equilibrium fluids, noise produces a small correction to the dynamics of large scale and long time time properties ($k \to 0, \omega \to 0$), the same is not true in one dimension [46, 47]. In addition, as we review below, the non-linear term that we dropped while linearizing the equations of motion (see Supplementary Information C) is no longer justified for the description of an equilibrium fluid in one dimension. (Although the packings are two-dimensional, their emergent hydrodynamic description is effectively one-dimensional because of the longitudinal binning

inherent in our description of the packing. This for instance ignores the effect of particles diffusing in the transverse directions.)

For simplicity, we consider the one dimensional Burger's equation stirred with a random force as a model for a one dimensional fluid-

$$\frac{\partial v}{\partial t} + v\frac{\partial v}{\partial x} = \nu\frac{\partial^2 v}{\partial x^2} - \lambda\frac{\partial \eta}{\partial x}, \tag{4.9}$$

where v is the fluid viscosity, ν is the kinematic viscosity and $\lambda\frac{\partial \eta}{\partial x}$ is the random stirring force such that in d-dimension (d=1 here):

$$\langle \eta(x,t)\rangle = 0 \tag{4.10}$$

$$\langle \eta(x,t)\eta(x',t')\rangle = 2D\delta^d(x-x')\delta(t-t'). \tag{4.11}$$

The Burger's equation (without random stirring) is obtained from the Navier-Stokes equation by ignoring the compressibility (pressure gradient term). As discussed earlier, the finite compressibility leads to propagating modes in the dispersion relation and the width of the power spectral density is measured in a frame that is moving at the speed of sound. Thus, the propagating modes only shifts the peak and do not effect the scaling properties of the width [47]. (Note, the Navier-Stokes equation is obtained from Newtons equations of motion written for a fluid particle. We can consider the Navier-Stokes with a noise term as the equivalent of a Langevin equation phenomenologically written for a fluid particle that is perturbed by thermal fluctuations.)

We can re-write this equation in terms of the potential function $v = -\lambda\frac{\partial \phi}{\partial x}$ to arrive at the Kardar-Parisi-Zhang (kpz) equation [48]:

$$\frac{\partial \phi}{\partial t} = \nu\frac{\partial^2 \phi}{\partial x^2} + \frac{\lambda}{2}\left(\frac{\partial \phi}{\partial x}\right)^2 + \eta. \tag{4.12}$$

Now consider rescaling the variables: $x \to bx'$, $t \to b^z t'$ and $\phi \to b^\xi \phi'$. In terms of the primed variables, Eq. (4.12) becomes [48]

$$\frac{\partial \phi}{\partial t} = b^{z-2}\nu\frac{\partial^2 \phi}{\partial x^2} + b^{\xi+z-2}\frac{\lambda}{2}\left(\frac{\partial \phi}{\partial x}\right)^2 + \eta', \tag{4.13}$$

where, $\eta' = b^{z-\xi}\eta(bx', b^z t')$ and therefore

$$\langle \eta'(x,t)\eta'(x',t')\rangle = 2Db^{z-d-2\xi}\delta^d(x-x')\delta(t-t'). \tag{4.14}$$

Therefore, the transport coefficients in the primed coordinates are $\nu' \to b^{z-2}\nu$,$\lambda' \to b^{\xi+z-2}\lambda$ and $D' \to b^{z-2\xi-d}D$.

Suppose, we now ignore the non-linear coefficient, that is $\lambda = 0$. Then, the transport coefficients are scale invariant for $z = 2$ and $\xi = \frac{(2-d)}{2}$. For this choice of exponents, we find the combination $\frac{x}{t^{\frac{1}{2}}}$ is invariant, as expected for ordinary diffusion.

However, around this point, λ scales as $b^{\frac{2-d}{2}}$. For $d < 2$, this is a relevant parameter and it is no longer possible to ignore the non-linear term. Thus, it is necessary for us to include both a fluctuating term and the non-linear term while describing equilibrium properties of a one dimensional fluid (d=2 is the critical dimension for fluids). By carrying out this analysis with the non-linear term and enforcing the invariance of λ under scale transformations (due to Galilean invariance of the Navier-Stokes equation) and of $D/\nu \sim k_B T$ (that scales as the equilibrium temperature of the fluid), we find the relevant exponents are $z = \frac{3}{2}, \xi = \frac{1}{2}$ [48, 47]. (Note, in this description the fluid itself is assumed not to be near a phase transition.)

With $z = \frac{3}{2}$, we therefore find the invariant combination to be $\frac{x}{t^{\frac{2}{3}}}$. The behaviour thus corresponds to a super-diffusive spreading of information, i.e.,

$$x^2 \sim t^{\frac{4}{3}}. \tag{4.15}$$

In order to see how super-diffusion effects the scaling of half-width with wave-number, we first define a time dependent diffusivity, i.e.,

$$x^2 \sim t^{\frac{4}{3}} = D(t)t \tag{4.16}$$

,where $D(t) \sim t^{\frac{1}{3}}$. The time correlation function associated with this diffusivity then scales as

$$C(t) \sim t^{\frac{1}{3}-1} = t^{-\frac{2}{3}} \tag{4.17}$$

since, $D \sim \int C(t)dt$. The Fourier transform of the time correlation function therefore scales as

$$C(\omega) \sim \omega^{-\frac{1}{3}} \tag{4.18}$$

For small wavenumbers near the linear regime of the dispersion curves $\omega \sim k$ and therefore, $C(k) \sim k^{-\frac{1}{3}}$. Since a transport

coefficient is associated with the low frequency limit of the correlation function in frequency space, i.e.,

$$D \sim \lim_{k\to 0} \int C(t) e^{-ikt} dt \tag{4.19}$$

$$\sim \lim_{k\to 0} C(k), \tag{4.20}$$

we find that the wave-number dependent diffusivity should scale as $D(k) \sim k^{-\frac{1}{3}}$. Consequently for small wave-numbers, the half-width scales as hw$\sim D(k)k^2 = k^{-\frac{1}{3}}k^2 = k^{\frac{5}{3}}$. This is close to the value we observe in simulations.

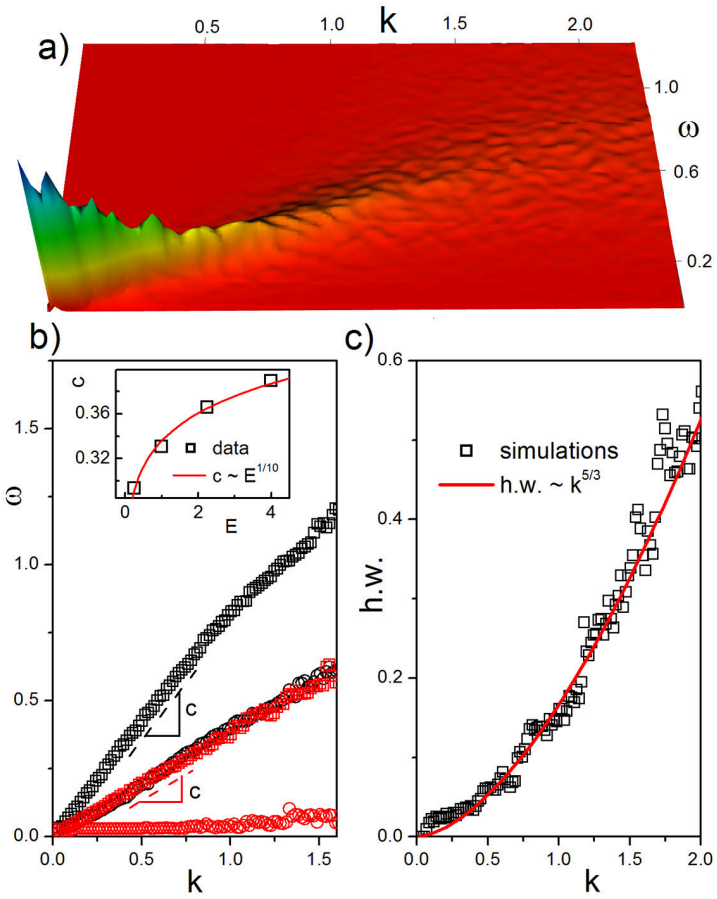

Figure 4.3: (a) The power spectral density for longitudinal modes that emerge in marginally compressed amorphous packings ($P \sim 10^{-6}$) by the complete disintegration of an initial solitary wave excitation. (b) The red squares shows the numerical data for the longitudinal dispersion curves. The slope of the linear regime scales with the energy of the solitary wave as $c \sim E^{\frac{1}{10}}$ for Hertzian interaction, that we identify with long wavelength longitudinal hydrodynamical modes. In contrast, the red circles shows the numerically obtained data for the transverse dispersion curve where no linear regime is seen. The shear mode is therefore non-propagating. For comparison, shown are linear dispersion curves for longitudinal (black squares) and transverse (black circles) obtained for highly compressed jammed packings, prepared at a pressure $P \sim 10^{-1}$.(c) The half-width obtained numerically from the longitudinal modes as a function of wavenumber on a linear scale and compared against the analytical estimates $h.w. \sim k^{\frac{5}{3}}$ (solid red line).

THERMAL FLUCTUATIONS

We found in the last chapter, that the attenuation of a solitary wave eventually leads to the emergence of an equilibrium like state, where particle fluctuations mimic thermal fluctuations. However, the system is not truly in a state of equilibrium, since there is no mechanism (such as an explicit coupling to a heat bath), to dampen external perturbations.

In this chapter, we therefore take a slight departure from our theme on the study of solitary wave propagation in disordered two dimensional packings and turn to the study of a strongly non-linear one dimensional chain of oscillators that is initially in the state of sonic vacuum, that we then couple to a heat bath. Like the granular analogue of temperature, thermal fluctuations induce an entropic rigidity. We then explore the propagation of a strongly non-linear solitary wave in this background of thermal fluctuations and environmental drag, and find an effective Langevin equation to describe the propagation of the solitary wave quasi-particle. This gives us the mean damping rate and thermal diffusion of the solitary wave quasi-particle that we compare against numerical results from a Langevin dynamic simulation. In addition, we find that a one dimensional chain composed of two sided non-linear springs, also supports an expansion solitary wave, as companion to the compressive solitary waves observed for macroscopic particles [†].

† The research ideas presented in this chapter evolved out of discussions with A.M. Turner and V. Vitelli and are part of Reference [62].